Programmable Quantum Simulations of Bosonic Systems with Trapped Ions

Or Katz[1,2,*] and Christopher Monroe[1,2,3,4]

[1]*Duke Quantum Center, Duke University, Durham, North Carolina 27701, USA*
[2]*Department of Electrical and Computer Engineering, Duke University, Durham, North Carolina 27708, USA*
[3]*Department of Physics, Duke University, Durham, North Carolina 27708, USA*
[4]*IonQ, Inc., College Park, Maryland 20740, USA*

Trapped atomic ion crystals are a leading platform for quantum simulations of spin systems, with programmable and long-range spin-spin interactions mediated by excitations of phonons in the crystal. We describe a complementary approach for quantum simulations of bosonic systems using phonons in trapped-ion crystals, here mediated by excitations of the trapped-ion spins. The scheme enables a high degree of programability across a dense graph of bosonic couplings, utilizing long-lived collective phonon modes in a trapped-ion chain. As such, it is well suited for tackling hard problems such as boson sampling and simulations of long-range bosonic and spin-boson Hamiltonians.

Bosons are identical particles whose quantum state is invariant to their exchange. This property governs phenomena such as Bose-Einstein condensation and photon bunching, forms the basis of continuous-variables quantum applications [1,2], and renders certain bosonic problems to be computationally hard, such as the longtime evolution of bosonic Hamiltonians [3,4] and the sampling of the distribution of interfering bosons [5]. While the boson sampling problem may be esoteric, it has attracted great interest as a quantum benchmark for challenging classical computing power [6].

Bosonic simulations have been demonstrated in various physical platforms using photons and atoms [7–17]. All of these platforms have been limited by either the programmable control and complexity of the bosonic interferometers or the extent of bosonic mode inputs to the interferometers. Ultracold bosonic atoms in optical lattices have been employed for simulation of various bosonic Hamiltonians and enabled the observation of various emergent phenomena [18–24]. While the number of bosonic particles and lattice sites can be large in this platform, the underlying hopping-type couplings between different sites is short range, which limits the class of models that can be efficiently simulated.

Phonons residing in *local* modes of trapped-ion crystals have also been proposed as a platform for simulation of bosonic Hamiltonians with short-range hopping terms and for boson sampling [25–30], with several demonstrations of interference, quantum walks, and blockade using a small number of ions and phonons [31–34]. Control over local phonon modes, however, requires considerable reduction of the trapping potential, which in turn limits the strength of hopping terms. These modes also exhibit a short lifetime that is limited by ion heating [33,35–37]. Trapped-ion

systems more naturally involve phonons representing *collective* normal modes of the entire crystal, coupled to the ions' internal state via radiation fields [38–41]. In this regime, the emergent spin-phonon couplings are nonlocal and densely connected, allowing programmability and control over a large class of spin-spin interactions spanning dozens or hundreds of spins and challenging classical computational simulation [42,43]. In this Letter, we propose an efficient scheme to generate a similarly large class of dense programmable bosonic "beam splitter" couplings between *long-lived* collective phonon modes in a trapped-ion crystal.

Trapped-ion quantum simulations of bosonic interactions and evolution consist of three stages: preparation, evolution under a target bosonic Hamiltonian, and detection. High-fidelity preparation of various nonclassical phononic states [44–49] and their faithful detection [50–53] have long been demonstrated in trapped-ion systems. While couplers between bosonic modes of a few trapped ions have been realized [36,54–57], the programming of efficient couplings between the many phonon modes in long ion chains remains an outstanding challenge, owing to the decoherence of phonons and fluctuations in the mode frequencies and drifts in the ion positions [35,37,45,58,59].

Here we propose a simple method to generate dense programmable beam splitter couplings between collective phonon modes in a trapped-ion crystal. The scheme operates in a dispersive regime of spin-boson interactions, akin to the root of trapped-ion quantum spin simulators [41,60]. But instead of exploiting geometric phases of phonon modes to create spin Hamiltonians, here we harness geometric phases of the spins in order to produce a large class of programmable bosonic Hamiltonians. We discuss the robustness of the method, demonstrate several simple

configurations, and consider the effects of dominant noise sources. We also demonstrate efficient preparation and detection protocols, and outline the scheme applicability for simulation of bosonic and spin-boson systems.

The collective phonon modes in a crystal of N trapped ions are determined by the external trapping potential and the Coulomb interaction between the ion charges. We represent each of the N phonon modes along the x principal axis using the bosonic creation and annihilation operators $\hat{a}_m^\dagger$ and $\hat{a}_m$ in the interaction picture, each rotating at its unique oscillation frequency ω_m. The external potential also determines the contribution of the ith ion to the motion of the mth mode, described by the orthonormal mode-participation matrix b_{im} [41].

The modes are coupled through the effective spin-1/2 systems hosted by internal electronic states of the ions. We consider the spin-phonon interaction realized by driving the ions on the first lower or "red" motional sideband transitions from the spin-flip carrier [54], using a radiation field with multiple tones as shown in Fig. 1. We assume $M \leq N$ ions are illuminated with control over the Rabi frequencies

(a)

(b)

(c)

$v_p - v_q = \omega_k - \omega_m$ $K_{k,m}$ red sidebands   tones   carrier

$-\omega_1$ $-\omega_k$ $-\omega_m$ $-\omega_N$ $-v_1$ $-v_p$ $-v_q$ $-v_P$ 0   Frequency

Δ

(d)

$K_{k-2,k+1}$
$K_{k-1,k+1}$
$K_{k,k+1}$
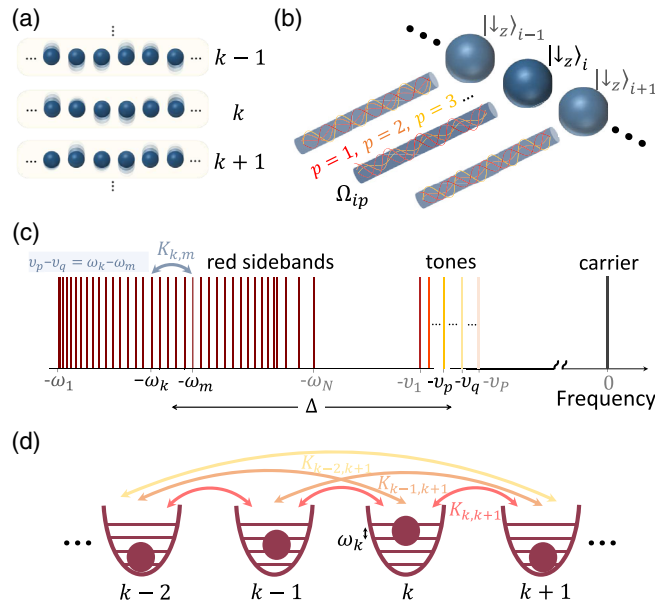ω_k

$k-2$ $k-1$ k $k+1$

FIG. 1. Quantum simulation of bosons. (a) Transverse collective modes of motion in a chain of N ions along one axis comprise a set of $1 \leq k \leq N$ decoupled bosonic modes hosting phonons. (b) Programmable coupling between the phonon modes is realized by driving $M \leq N$ spin-down ions with $P \leq N$ tones near the red-sideband transitions in the dispersive regime (see text). (c) Calculated red-sideband mode spectrum for a chain of 40 equidistant ions. Exemplary P tones are detuned by Δ from the mode spectrum to suppress spin-phonon excitations. Hopping amplitude K_{km} between the k and m motional modes with frequencies ω_k and ω_m is generated predominantly by pairs of tones p and q with frequencies v_p and v_q which satisfy the resonance condition $\omega_k - \omega_m = v_p - v_q$. (d) The emergent coupling between normal phonon modes manifest as the programmable hopping amplitudes K_{km}, using the ion spins as a quantum bus.

$\Omega_i(t)$ proportional to the drive strength at the position of the i ion, and represent the drive by a superposition of $P \leq N$ tones as $\Omega_i(t) = \sum_p \Omega_{ip} e^{-i v_p t} + \text{H.c.}$. For simplicity, we assume a constant (complex) amplitude matrix Ω_{ip} [74] and uniform red detunings $v_p > 0$ over all illuminated ions. We assume the field drives predominantly the red sidebands $(|\omega_m - v_p| \ll \omega_m)$ and that motion is confined within the Lamb-Dicke regime $[\sum_m \eta_m^2 b_{im}^2 \langle (\hat{a}_m^\dagger + \hat{a}_m)^2 \rangle]^{1/2} \ll 1$, where $\eta_m = K\sqrt{\hbar/2\mathcal{M}\omega_m}$. Here, K denotes the effective wave number of the driving field aligned with the x axis and $\mathcal{M}$ the mass of a single ion. Under these conditions, the time-dependent spin-phonon interaction is given by the multi-mode off-resonance Jaynes-Cummings Hamiltonian [75],

$$H_{\text{rsb}} = \frac{i\hbar}{2} \sum_{i,m,p} \eta_{im} \Omega_{ip} e^{-i\Delta_{pm} t} \hat{\sigma}_+^{(i)} \hat{a}_m + \text{H.c.}, \qquad (1)$$

where $\hat{\sigma}_\pm^{(i)}$ are the Pauli spin-flip operators of ion i, $\Delta_{pm} = \omega_m - v_p$ is the detuning of tone p from the red sideband of mode m, and $\eta_{im} = \eta_m b_{im}$.

The Hamiltonian in Eq. (1) describes the usual exchange of excitations between spins and phonons, where absorption (emission) of a phonon into one of the normal modes is correlated with flipping one of the spins upward (downward). We consider the dispersive regime for which direct spin-phonon exchange is considerably suppressed owing to the large detuning of the drive, characterized by the parameter $\varepsilon_{mp}^{(i)} \equiv \eta_{im}\Omega_{ip}/\Delta_{pm} \ll 1$. We can derive the time-evolution operator of spins and phonons under Eq. (1) through the Magnus expansion, consisting of a sequence of nested commutators of the Hamiltonian with itself at different times [41]. While the expansion does not truncate, we find that the dominant contribution to the evolution from the lowest order in $\varepsilon_{mp}^{(i)}$ arises from the second term in the Magnus expansion [61], and the evolution operator at time T takes the form

$$U(T) = \exp\left[-\frac{i}{\hbar}(H_s + H_p)T + \epsilon\right]. \qquad (2)$$

The evolution is thus well described by two effective Hamiltonians, H_s and H_p. The additional operator ϵ encompasses a small error to the simulation output due to residual spin-phonon coupling, discussed further in Supplemental Material (SM) [61].

The first effective Hamiltonian term is

$$H_s = -\sum_{i,j} J_{ij}(\hat{\sigma}_+^{(i)}\hat{\sigma}_-^{(j)} + \hat{\sigma}_-^{(i)}\hat{\sigma}_+^{(j)}), \qquad (3)$$

describing nonlocal hopping of spins with hopping matrix J_{ij} between spins i and j. For long evolution times T, given

sufficient spectral resolution between pairs of tones p, q, or $|\nu_p - \nu_q|T \gg 1$, the matrix J_{ij} is given by [61]

$$J_{ij} = \frac{1}{8} \sum_{m=1}^{N} \sum_{p=1}^{P} \frac{\eta_{im}\eta_{jm}\Omega_{ip}^*\Omega_{jp}}{\Delta_{pm}}. \quad (4)$$

This matrix is similar to the spin-spin couplings that emerge in trapped-ion based quantum spin simulators, featuring a tunable interaction range and full programmability [40,41,74].

The second effective Hamiltonian term is

$$H_p = -\sum_{k,m,i} K_{km}^{(i)} \hat{a}_k \hat{a}_m^\dagger \hat{\sigma}_z^{(i)}, \quad (5)$$

describing spin-dependent hopping of phonons between pairs of modes, or equivalently, phonon-dependent Stark shifts. The matrix element $K_{km}^{(i)}$ describes the hopping amplitude between the m and k modes that is generated by driving spin i. For long evolution times Δ_{pm}, the hopping amplitudes are given by [61]

$$K_{km}^{(i)} = \sum_{p,q} \frac{\eta_{ik}\eta_{im}\Omega_{iq}\Omega_{ip}^*(\Delta_{qm} + \Delta_{pk})}{8\Delta_{pk}\Delta_{qm}} \tilde{\delta}_{\Delta_{qm},\Delta_{pk}}, \quad (6)$$

where the time-dependent function,

$$\tilde{\delta}_{\Delta_{qm},\Delta_{pk}} = e^{(i/2)(\Delta_{qm}-\Delta_{pk})T} \mathrm{sinc}\left[\frac{1}{2}(\Delta_{qm} - \Delta_{pk})T\right], \quad (7)$$

with $\mathrm{sinc}(x) \equiv \sin x/x$. For sufficiently long evolution times considered here, $\tilde{\delta}_{\Delta_{qm},\Delta_{pk}}$ acts approximately like a Kronecker delta function. This is essentially energy conservation, as only pairs of tones p, q whose frequency difference are resonant with the freequency difference between the k, m modes ($\Delta_{pk} = \Delta_{qm}$) give a sizable contribution to the boson hopping amplitude in Eq. (6), as illustrated in Fig. 1.

We find that the error term in Eq. (2) is given by (see SM [61])

$$\epsilon = \sum_{i,m,p} \varepsilon_{mp}^{(i)} \hat{\sigma}_+^{(i)} \hat{a}_m e^{-(i/2)\Delta_{pm}T} \sin\left(\frac{\Delta_{pm}T}{2}\right) + \mathrm{H.c.}, \quad (8)$$

describing spin flips which are correlated with emission or absorption of phonons. Unlike the secular terms in the evolution of Eq. (2), whose contributions increase linearly in time and correspond to effective Hamiltonians H_s and H_p, the contribution of the error term is small and bounded in time.

To generate a beam splitter interaction between the collective phonon modes in the trapped-ion crystal, we focus our discussion on initial states for which spin and phonons are disentangled, and specifically, with all spins pointing down. The system wave function can then be cast as $|\downarrow_{1z}, \ldots, \downarrow_{Nz}\rangle \otimes |\chi\rangle$ for any initial phononic state $|\chi\rangle$. Such initialization can be efficiently realized via standard sideband cooling and optical pumping schemes [76,77]. This configuration determines the sign of the phonon-hopping terms in Eq. (5), and casts H_p as the bosonic beam splitter Hamiltonian,

$$H_{\mathrm{BS}} = \sum_{k,m} K_{km} \hat{a}_k \hat{a}_m^\dagger, \quad (9)$$

with hopping terms,

$$K_{km} = -\sum_i \langle \hat{\sigma}_z^{(i)} \rangle K_{km}^{(i)} = \sum_i K_{km}^{(i)}, \quad (10)$$

for $\langle \hat{\sigma}_z^{(i)} \rangle = -1$. Furthermore, this particular choice eliminates the effect of H_s on the simulation, which could otherwise flip spins and temporally change the couplings K_{km} via $\langle \hat{\sigma}_z^{(i)} \rangle$. Here, hopping between different pairs of spins $i \neq j$ is forbidden since $\hat{\sigma}_-^{(i)}|\downarrow_i\rangle = 0$, and terms with $i = j$ only append a global phase that is independent of the phonon state.

The Hermitian beam splitter matrix K_{km} in Eq. (9) contains $N(N-1)/2$ unique elements which can be programmed by the $MP \leq N^2$ control parameters of the matrix Ω_{ip} in Eq. (6). Thus, the control parameters for a target matrix K_{km} can be found using standard optimization techniques, similar to the techniques used for simulations of spin systems [74].

We now present a few examples of K_{km} that are efficiently calculated for simple Rabi frequency matrices Ω_{ip}, satisfying $MP \ll N^2$. We consider a linear chain of $N = 40$ ions with typical experimental parameters: We assume a radial center of mass trap frequency of $\omega_r = 4$ MHz for which $\eta_m \approx 0.1$, drive amplitude of $\Omega_0 = 200 - 300$ kHz for a few selected tones and ions, a detuning of $\Delta = 400$ kHz from the middle of the red-sideband spectrum and a (short) simulation time of $T = 1$ ms. The electrostatic axial trap potential is composed of a quadratic and quartic terms set to produce a nearly equidistant spacing between the ions of about 3.6 μm [78], mainly to ease access by an equidistant array of beams [79–81]. Interestingly, this potential also renders the spacing between the frequencies of the central modes to be approximately equidistant, as shown in Fig. 1. The constant spacing (of about 8.5 kHz) enables efficient simultaneous coupling to multiple modes using a small set of tones. As the central radial modes feature low heating rates and high mode stability [82–84], we choose to program the couplings between the central 20 modes, which are well isolate from the edge modes. Detailed parameters and the full beam splitter matrices are provided in Ref. [61].
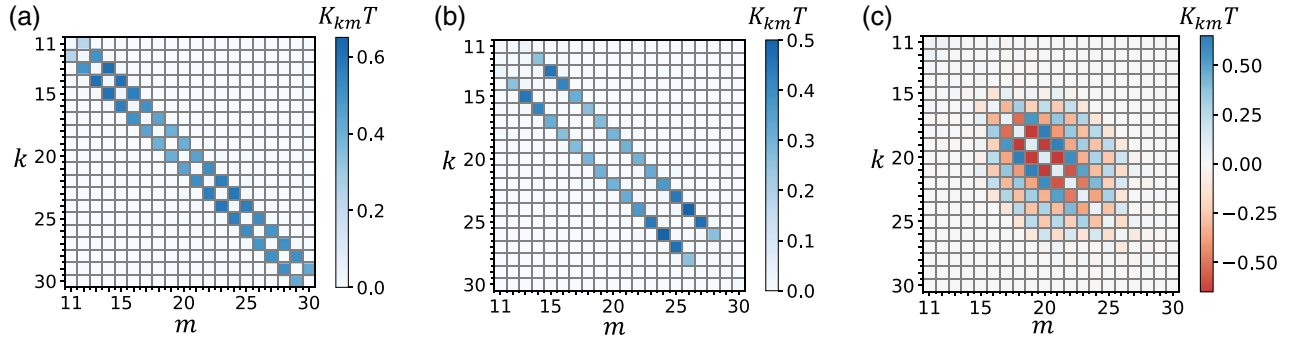
FIG. 2. Programmable bosonic hopping matrix. Exemplary coupling between the 20 central phonon modes in a $N = 40$ ions chain for $T = 1$ ms. (a) Nearest-neighbor coupling is realized via illumination of four ions ($2 \leq i \leq 5$) with two in-phase tones whose relative frequencies match the average frequency spacing between modes. (b) Next-nearest-neighbor coupling using the same configuration but doubling the relative frequency between the two tones. (c) Long-range coupling via illumination of a single ion ($i = 3$) with six tones. Staggered-sign amplitudes are realized by shifting the phase of odd tones by π. The calculation uses Eq. (7) and does not assume any frequency selectivity. On-site terms are suppressed in (a)–(c) by driving the ions with an additional single tone near the blue sidebands, and other unwanted couplings are very small; see Ref. [61].

First we consider uniform driving of all ions, where $M = N$ and Ω_{ip} is independent of i. Summation over the contribution of all ions in Eq. (10) renders K_{km} diagonal with no intermode hopping, owing to the orthogonality of the mode-participation matrix $\sum_i b_{ik} b_{im} = \delta_{km}$. Such on-site hopping terms can be controllably suppressed, if necessary, by driving an additional single tone near the blue-sideband transition [61]. This simple technique is applied in the following examples.

In Fig. 2(a) we present K_{km} with hopping terms predominantly between (spectrally) nearest-neighbor modes, illuminating only $M = 4$ ions ($2 \leq i \leq 5$) with two (in-phase) tones near the red sidebands, choosing their frequency difference to be $\nu_2 - \nu_1 \approx 8.5$ kHz. In Fig. 2(b) we present K_{km} with hopping terms predominantly between the next-nearest-neighbor modes, using the same configuration but doubling the relative frequency of the two tones ($\nu_2 - \nu_1 \approx 17$ kHz). These examples illustrate the crucial role of $\tilde{\delta}$ in Eq. (7), which enables efficient and simple engineering of the hopping terms via control over the tone spectrum. The residual couplings between other modes, and particularly to the rapidly heating center-of-mass mode, are very small [61]. Finally, in Fig. 2(c) we present the beam splitter matrix K_{km} realized by illuminating a single ion ($i = 3$) using six tones, demonstrating long-range hopping amplitudes. Here we realize staggering amplitudes by setting $\Omega_{ip} = \Omega_0 \delta_{i3}(-1)^p$, i.e., shifting the relative phase between the odd and even tones by π. Notably, the hopping terms are not limited to real values and can take complex values via tuning of the relative phase between the tones. Importantly, the relative phase between tones at each ion requires neither interferometric stability nor control over the optical phase between different beams; instead, the necessary phase control can be achieved via simple low frequency modulation of each beam, e.g., with acusto-optical modulators [79–81].

We can analyze the scaling of light-induced error and hopping terms with the chain length by assuming $\eta_{im} \sim \eta/\sqrt{N}$ for the Lamb-Dicke parameters. For typical Rabi frequencies Ω and detuning Δ with $\epsilon = \eta\Omega/\Delta$ and $\epsilon \ll 1$, the probability for error scales as $MP\epsilon^2/N$ per mode [Eq. (8)]. In the dispersive regime, the typical hopping amplitude is given by $MP\epsilon^2\Delta/N$, where $\Delta T \gg 1$ is the ratio between the hopping-accumulated phase and light-induced noise. Although this ratio is independent of N,
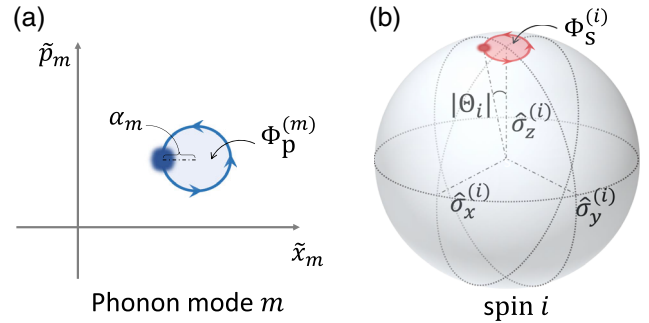

FIG. 3. Geometric phase-gate interpretation. The evolution of spins and phonons by Hamiltonians H_s and H_p emerges from simultaneous accumulation of geometric phases in the phonon's phase space (a) and spin's Bloch sphere (b). (a) Illustrative trajectory of the phonon state in phase space of mode m, where $\tilde{x}_m = (\hat{a}_m + \hat{a}_m^\dagger)/2$ and $\tilde{p}_m = i(\hat{a}_m^\dagger - \hat{a}_m)/2$ [85,86]. The state moves in loops by the *spin-dependent* displacement α_m, enclosing the area that corresponds to the geometric phase $\Phi_p^{(m)}$ which is associated with the spin-hopping Hamiltonian H_s. (b) The spin of ion i is rotated in loops by the *phonon-dependent* angle Θ_i, enclosing the area on the Bloch sphere that corresponds to the geometric phase $\Phi_s^{(i)}$, which is associated with the phonon-hopping Hamiltonian H_p. The total phase appended to the quantum state $\sum_i \Phi_s^{(i)} + \sum_m \Phi_p^{(m)}$ yields the spin-spin and phonon-phonon hopping Hamiltonians in Eqs. (3) and (5).

increasing the simulation time T linearly with N compensates for the decrease in frequency spacing and hopping amplitudes, which are inversely proportional to N. See Ref. [61] for more details.

We now compare the timescale of coherent evolution with that of noise mechanisms. Coherent evolution time is usually determined by when $K_{km}T$ equals one, which takes around 1 ms for the aforementioned 40-ion chain example. In Ref. [61] we examine motional decoherence caused by heating, confinement noise, and light coupling. Electric field noise, which changes slowly across the ion chain, does not heat most collective modes, as it couples poorly to modes whose participation factors change quickly. Confinement noise has little impact on the relative dephasing between collective phonon modes, because it originates from a common source. Small light-induced errors can be efficiently detected and excluded. Our analysis concludes that most collective modes away from the center-of-mass mode have coherence times of over 1 s under feasible experimental conditions, at least 3 orders of magnitude greater than simulation time. In contrast, techniques using local phonon modes are essentially limited by the much faster heating rate of one ion.

The scheme proposed here can be applied for simulation of a large variety of bosonic models. The nonlocal nature of the collective phonons naturally allows the simulation of bosonic Hamiltonians featuring long-range hopping amplitudes [4,5]. The proposed method also enables universal and efficient programming of beam splitter matrices for the boson sampling problem [6], realization of topological phases [87], and potentially computation using continuous and discrete variables [36,57,88]. These applications also require efficient initialization and detection. While both have been demonstrated for a few phonon modes [29,36,45], in Ref. [61] we demonstrate numerically simultaneous and high-fidelity preparation and detection of phonons in multiple modes, within about 1 ms for the 40-ion chain configuration.

The scheme can also be used for simulation of various spin-boson models, which are expected to manifest emergent phenomena [89–92]. Potentially, spin-boson couplings can be realized by resonant driving one subset of ions on the red or blue sideband transitions [93], while hopping between phonon modes can be realized by illumination of another subset of ions with multiple tones in the dispersive regime. In the Supplemental Material [61], we discuss the implementation of the Jaynes-Cummings-Hubbard [89,90] and the Hubbard-Rabi [92] models using the scheme reported above.

Before concluding, we find it insightful to highlight the physical mechanism that enables the simulation of bosonic Hamiltonians and generates the evolution in Eq. (2). Using the Heisenberg picture, we can illustrate the simultaneous action of the red-sideband Hamiltonian [Eq. (1)] in the phase space of the phononic modes and the spins' Bloch sphere, as shown in Fig. 3. In the phase space of mode m, the phononic state is displaced in small loops by *spin-dependent displacement* $\alpha_m(t) = -\frac{1}{2}\int_0^t \sum_{ip} \varepsilon_{mp}^{(i)*} e^{-i\delta_{pm}\tau} \hat{\sigma}_+^{(i)}(\tau)d\tau$. At long evolution times, the loops are traversed numerously and accumulate a sizable phase-space area that corresponds to a geometric phase $\Phi_p^{(m)}(T) = (i/4)\int_0^T (\alpha_m^\dagger \dot{\alpha}_m - \alpha_m \dot{\alpha}_m^\dagger)dt$ that is appended to the quantum state. The total geometric phase enclosed by all modes $(\sum_m \Phi_p^{(m)})$ then yields the evolution governed by the effective Hamiltonian H_s in Eq. (3), when considering the dispersive regime for which high order correlations between the spins and motion are negligible [61].

Concurrently, the spin state of ion i is rotated as a function of time in small loops around the pole of the Bloch sphere by the *phonon-dependent angle* $\Theta_i(t) = -\sum_{p,m}\int_0^t \varepsilon_{mp}^{(i)*} e^{-i\delta_{pm}\tau}\hat{a}_m^\dagger(\tau)d\tau$, which corresponds to the rotation angles $\Theta_i = \theta_x^{(i)} + i\theta_y^{(i)}$. At long evolution times, these loops are traversed numerously and accumulate a sizable area that corresponds to a geometric phase $\Phi_s^{(i)} = (i/4)\int_0^T (\Theta_i^\dagger \dot{\Theta}_i - \Theta_i \dot{\Theta}_i^\dagger)\hat{\sigma}_z^{(i)}dt$ that is appended to the quantum state. Intriguingly, the operator $\hat{\sigma}_z^{(i)}$ emerges here owing to the curvature of the Bloch sphere. The total geometric phase enclosed by all ions $\sum_i \Phi_s^{(i)}$ then corresponds to the evolution governed by the effective Hamiltonian H_p in Eq. (5), when neglecting high order correlations between the spins and motion in the dispersive regime [61]. We therefore conclude that our scheme realizes boson-boson couplings by geometric phase gates, accumulated over the Bloch spheres of ion spins.

*Corresponding author.
or.katz@duke.edu

[1] S. Braunstein and P. van Loock, Rev. Mod. Phys. **77**, 513 (2005).

[2] C. Weedbrook, S. Pirandola, R. García-Patrón, N. J. Cerf, T. C. Ralph, J. H. Shapiro, and S. Lloyd, Rev. Mod. Phys. **84**, 621 (2012).

[3] A. Deshpande, B. Fefferman, M. C. Tran, M. Foss-Feig, and A. V. Gorshkov, Phys. Rev. Lett. **121**, 030501 (2018).

[4] N. Maskara, A. Deshpande, A. Ehrenberg, M. C. Tran, B. Fefferman, and A. V. Gorshkov, Phys. Rev. Lett. **129**, 150604 (2022).

[5] S. Aaronson and A. Arkhipov, in *Proceedings of the Forty-Third Annual ACM Symposium on Theory of computing* (Association for Computing Machinery, 2011), pp. 333–342, 10.1145/1993636.1993682.

[6] A. P. Lund, M. J. Bremner, and T. C. Ralph, npj Quantum Inf. **3**, 15 (2017).

[7] N. Spagnolo, C. Vitelli, M. Bentivegna, D. J. Brod, A. Crespi, F. Flamini, S. Giacomini, G. Milani, R. Ramponi, P. Mataloni *et al.*, Nat. Photonics **8**, 615 (2014).

[8] M. Bentivegna, N. Spagnolo, C. Vitelli, F. Flamini, N. Viggianiello, L. Latmiral, P. Mataloni, D. J. Brod, E. F. Galvão, A. Crespi *et al.*, Sci. Adv. **1**, e1400255 (2015).

[9] B. Peropadre, G. G. Guerreschi, J. Huh, and A. Aspuru-Guzik, Phys. Rev. Lett. **117**, 140505 (2016).

[10] J. C. Loredo, M. A. Broome, P. Hilaire, O. Gazzano, I. Sagnes, A. Lemaitre, M. P. Almeida, P. Senellart, and A. G. White, Phys. Rev. Lett. **118**, 130503 (2017).

[11] Y. Y. Gao, B. J. Lester, Y. Zhang, C. Wang, S. Rosenblum, L. Frunzio, L. Jiang, S. M. Girvin, and R. J. Schoelkopf, Phys. Rev. X **8**, 021073 (2018).

[12] H. Wang, J. Qin, X. Ding, M.-C. Chen, S. Chen, X. You, Y.-M. He, X. Jiang, L. You, Z. Wang *et al.*, Phys. Rev. Lett. **123**, 250503 (2019).

[13] H.-S. Zhong, H. Wang, Y.-H. Deng, M.-C. Chen, L.-C. Peng, Y.-H. Luo, J. Qin, D. Wu, X. Ding, Y. Hu *et al.*, Science **370**, 1460 (2020).

[14] H.-S. Zhong, Y.-H. Deng, J. Qin, H. Wang, M.-C. Chen, L.-C. Peng, Y.-H. Luo, D. Wu, S.-Q. Gong, H. Su *et al.*, Phys. Rev. Lett. **127**, 180502 (2021).

[15] C. S. Wang, J. C. Curtis, B. J. Lester, Y. Zhang, Y. Y. Gao, J. Freeze, V. S. Batista, P. H. Vaccaro, I. L. Chuang, L. Frunzio *et al.*, Phys. Rev. X **10**, 021060 (2020).

[16] L. S. Madsen, F. Laudenbach, M. F. Askarani, F. Rortais, T. Vincent, J. F. F. Bulmer, F. M. Miatto, L. Neuhaus, L. G. Helt, M. J. Collins, A. E. Lita, T. Gerrits, S. W. Nam, V. D. Vaidya, M. Menotti, I. Dhand, Z. Vernon, N. Quesada, and J. Lavoie, Nature (London) **606**, 75 (2022).

[17] A. W. Young, W. J. Eckner, N. Schine, A. M. Childs, and A. M. Kaufman, Science **377**, 885 (2022).

[18] D. Jaksch, C. Bruder, J. I. Cirac, C. W. Gardiner, and P. Zoller, Phys. Rev. Lett. **81**, 3108 (1998).

[19] I. Bloch, J. Dalibard, and S. Nascimbene, Nat. Phys. **8**, 267 (2012).

[20] F. Schäfer, T. Fukuhara, S. Sugawa, Y. Takasu, and Y. Takahashi, Nat. Rev. Phys. **2**, 411 (2020).

[21] M. Greiner, O. Mandel, T. Esslinger, T. W. Hänsch, and I. Bloch, Nature (London) **415**, 39 (2002).

[22] S. Trotzky, Y.-A. Chen, A. Flesch, I. P. McCulloch, U. Schollwöck, J. Eisert, and I. Bloch, Nat. Phys. **8**, 325 (2012).

[23] J.-y. Choi, S. Hild, J. Zeiher, P. Schauß, A. Rubio-Abadal, T. Yefsah, V. Khemani, D. A. Huse, I. Bloch, and C. Gross, Science **352**, 1547 (2016).

[24] S. Braun, M. Friesdorf, S. S. Hodgman, M. Schreiber, J. P. Ronzheimer, A. Riera, M. Del Rey, I. Bloch, J. Eisert, and U. Schneider, Proc. Natl. Acad. Sci. U.S.A. **112**, 3641 (2015).

[25] H.-K. Lau and D. F. V. James, Phys. Rev. A **85**, 062329 (2012).

[26] D. Porras and J. I. Cirac, Phys. Rev. Lett. **93**, 263602 (2004).

[27] X.-L. Deng, D. Porras, and J. I. Cirac, Phys. Rev. A **77**, 033403 (2008).

[28] A. Serafini, A. Retzker, and M. B. Plenio, New J. Phys. **11**, 023007 (2009).

[29] C. Shen, Z. Zhang, and L.-M. Duan, Phys. Rev. Lett. **112**, 050504 (2014).

[30] A. Bermudez, M. Martin-Delgado, and D. Porras, New J. Phys. **12**, 123016 (2010).

[31] K. Toyoda, R. Hiji, A. Noguchi, and S. Urabe, Nature (London) **527**, 74 (2015).

[32] M. Tamura, T. Mukaiyama, and K. Toyoda, Phys. Rev. Lett. **124**, 200501 (2020).

[33] S. Debnath, N. M. Linke, S.-T. Wang, C. Figgatt, K. A. Landsman, L.-M. Duan, and C. Monroe, Phys. Rev. Lett. **120**, 073001 (2018).

[34] H. Schmitz, R. Matjeschk, C. Schneider, J. Glueckert, M. Enderlein, T. Huber, and T. Schaetz, Phys. Rev. Lett. **103**, 090504 (2009).

[35] M. Brownnutt, M. Kumph, P. Rabl, and R. Blatt, Rev. Mod. Phys. **87**, 1419 (2015).

[36] W. Chen, J. Gan, J.-N. Zhang, D. Matuskevich, and K. Kim, Chin. Phys. B **30**, 060311 (2021).

[37] M. Cetina, L. N. Egan, C. Noel, M. L. Goldman, D. Biswas, A. R. Risinger, D. Zhu, and C. Monroe, PRX Quantum **3**, 010334 (2022).

[38] J. I. Cirac and P. Zoller, Phys. Rev. Lett. **74**, 4091 (1995).

[39] D. Porras and J. I. Cirac, Phys. Rev. Lett. **92**, 207901 (2004).

[40] C. Schneider, D. Porras, and T. Schaetz, Rep. Prog. Phys. **75**, 024401 (2012).

[41] C. Monroe, W. C. Campbell, L.-M. Duan, Z.-X. Gong, A. V. Gorshkov, P. W. Hess, R. Islam, K. Kim, N. M. Linke, G. Pagano, P. Richerme, C. Senko, and N. Y. Yao, Rev. Mod. Phys. **93**, 025001 (2021).

[42] J. Zhang, G. Pagano, P. W. Hess, A. Kyprianidis, P. Becker, H. Kaplan, A. V. Gorshkov, Z.-X. Gong, and C. Monroe, Nature (London) **551**, 601 (2017).

[43] J. W. Britton, B. C. Sawyer, A. C. Keith, C.-C. J. Wang, J. K. Freericks, H. Uys, M. J. Biercuk, and J. J. Bollinger, Nature (London) **484**, 489 (2012).

[44] D. M. Meekhof, C. Monroe, B. E. King, W. M. Itano, and D. J. Wineland, Phys. Rev. Lett. **76**, 1796 (1996).

[45] K. C. McCormick, J. Keller, S. C. Burd, D. J. Wineland, A. C. Wilson, and D. Leibfried, Nature (London) **572**, 86 (2019).

[46] J. Zhang, M. Um, D. Lv, J.-N. Zhang, L.-M. Duan, and K. Kim, Phys. Rev. Lett. **121**, 160502 (2018).

[47] A. Ben-Kish, B. DeMarco, V. Meyer, M. Rowe, J. Britton, W. M. Itano, B. Jelenković, C. Langer, D. Leibfried, T. Rosenband, and D. J. Wineland, Phys. Rev. Lett. **90**, 037902 (2003).

[48] D. Kienzler, H.-Y. Lo, V. Negnevitsky, C. Flühmann, M. Marinelli, and J. P. Home, Phys. Rev. Lett. **119**, 033602 (2017).

[49] C. Flühmann, T. L. Nguyen, M. Marinelli, V. Negnevitsky, K. Mehta, and J. Home, Nature (London) **566**, 513 (2019).

[50] S. An, J.-N. Zhang, M. Um, D. Lv, Y. Lu, J. Zhang, Z.-Q. Yin, H. Quan, and K. Kim, Nat. Phys. **11**, 193 (2015).

[51] M. Um, J. Zhang, D. Lv, Y. Lu, S. An, J.-N. Zhang, H. Nha, M. Kim, and K. Kim, Nat. Commun. **7**, 1 (2016).

[52] C. Flühmann and J. P. Home, Phys. Rev. Lett. **125**, 043602 (2020).

[53] S. Ding, G. Maslennikov, R. Hablützel, and D. Matsukevich, Phys. Rev. Lett. **119**, 193602 (2017).

[54] D. Leibfried, B. DeMarco, V. Meyer, M. Rowe, A. Ben-Kish, J. Britton, W. M. Itano, B. Jelenković, C. Langer, T. Rosenband *et al.*, Phys. Rev. Lett. **89**, 247901 (2002).

[55] Y. Shen, Y. Lu, K. Zhang, J. Zhang, S. Zhang, J. Huh, and K. Kim, Chem. Sci. **9**, 836 (2018).

[56] S. Ding, G. Maslennikov, R. Hablützel, and D. Matsukevich, Phys. Rev. Lett. **121**, 130502 (2018).

[57] H. C. J. Gan, G. Maslennikov, K.-W. Tseng, C. Nguyen, and D. Matsukevich, Phys. Rev. Lett. **124**, 170502 (2020).

[58] L. Deslauriers, S. Olmschenk, D. Stick, W. K. Hensinger, J. Sterk, and C. Monroe, Phys. Rev. Lett. **97**, 103007 (2006).

[59] A. R. Milne, C. Hempel, L. Li, C. L. Edmunds, H. J. Slatyer, H. Ball, M. R. Hush, and M. J. Biercuk, Phys. Rev. Lett. **126**, 250506 (2021).

[60] L. Feng, O. Katz, C. Haack, M. Maghrebi, A. V. Gorshkov, Z. Gong, M. Cetina, and C. Monroe, arXiv:2211.01275.

[61] See Supplemental Material at http://link.aps.org/supplemental/10.1103/PhysRevLett.131.033604, which includes includes Refs. [63–74], for analysis of the main motional noise sources and comparison to the coherent evolution timescale, the derivation of the unitary evolution operator, compensation of on-site hopping terms using blue-sideband transition, the full beam splitter matrices estimation of residual couplings, numerical demonstration of simultaneous preparation and detection protocols, discussion on spin-boson models, and derivation of the geometric phase using the Heisenberg picture.

[62] Q. A. Turchette, C. J. Myatt, B. E. King, C. A. Sackett, D. Kielpinski, W. M. Itano, C. Monroe, and D. J. Wineland, Phys. Rev. A **62**, 053807 (2000).

[63] D. Kalincev, L. Dreissen, A. Kulosa, C. Yeh, H. Fürst, and T. Mehlstäubler, Quantum Sci. Technol. **6**, 034003 (2021).

[64] V. Jarlaud, P. Hrmo, M. K. Joshi, and R. C. Thompson, J. Phys. B **54**, 015501 (2020).

[65] G. G. K. Simon, Measuring trapped-ion motional decoherence through direct manipulation of motional coherent states, Ph. D. thesis, Massachusetts Institute of Technology, 2020.

[66] W. Morong, K. S. Collins, A. De, E. Stavropoulos, T. You, and C. Monroe, PRX Quantum **4**, 010334 (2023).

[67] D. J. Wineland, C. Monroe, W. M. Itano, D. Leibfried, B. E. King, and D. M. Meekhof, J. Res. Natl. Inst. Stand. Technol. **103**, 259 (1998).

[68] J.-S. Chen, K. Wright, N. C. Pisenti, D. Murphy, K. M. Beck, K. Landsman, J. M. Amini, and Y. Nam, Phys. Rev. A **102**, 043110 (2020).

[69] N. Quesada, J. M. Arrazola, and N. Killoran, Phys. Rev. A **98**, 062322 (2018).

[70] J. F. F. Bulmer, S. Paesani, R. S. Chadwick, and N. Quesada, Phys. Rev. A **106**, 043712 (2022).

[71] H. Wang, Y. He, Y.-H. Li, Z.-E. Su, B. Li, H.-L. Huang, X. Ding, M.-C. Chen, C. Liu, J. Qin *et al.*, Nat. Photonics **11**, 361 (2017).

[72] O. Katz, L. Feng, A. Risinger, C. Monroe, and M. Cetina, Nat. Phys. (2023).

[73] C.-C. Joseph Wang and J. Freericks, Phys. Rev. A **86**, 032329 (2012).

[74] S. Korenblit, D. Kafri, W. C. Campbell, R. Islam, E. E. Edwards, Z.-X. Gong, G.-D. Lin, L.-M. Duan, J. Kim, K. Kim *et al.*, New J. Phys. **14**, 095024 (2012).

[75] D. Leibfried, R. Blatt, C. Monroe, and D. Wineland, Rev. Mod. Phys. **75**, 281 (2003).

[76] C. K. Law and J. H. Eberly, Phys. Rev. Lett. **76**, 1055 (1996).

[77] A. Ben-Kish, B. DeMarco, V. Meyer, M. Rowe, J. Britton, W. M. Itano, B. M. Jelenković, C. Langer, D. Leibfried, T. Rosenband, and D. J. Wineland, Phys. Rev. Lett. **90**, 037902 (2003).

[78] G.-D. Lin, S.-L. Zhu, R. Islam, K. Kim, M.-S. Chang, S. Korenblit, C. Monroe, and L.-M. Duan, Europhys. Lett. **86**, 60004 (2009).

[79] K. Wright, K. M. Beck, S. Debnath, J. Amini, Y. Nam, N. Grzesiak, J.-S. Chen, N. Pisenti, M. Chmielewski, C. Collins *et al.*, Nat. Commun. **10**, 1 (2019).

[80] D. Zhu, G. D. Kahanamoku-Meyer, L. Lewis, C. Noel, O. Katz, B. Harraz, Q. Wang, A. Risinger, L. Feng, D. Biswas, L. Egan, A. Gheorghiu, Y. Nam, T. Vidick, U. Vazirani, N. Y. Yao, M. Cetina, and C. Monroe, arXiv:2112.05156.

[81] L. Egan, D. M. Debroy, C. Noel, A. Risinger, D. Zhu, D. Biswas, M. Newman, M. Li, K. R. Brown, M. Cetina *et al.*, Nature (London) **598**, 281 (2021).

[82] S.-L. Zhu, C. Monroe, and L.-M. Duan, Phys. Rev. Lett. **97**, 050505 (2006).

[83] L. N. Egan, Scaling quantum computers with long chains of trapped ions, Ph.D. thesis, University of Maryland, College Park, 2021.

[84] R. Lechner, Multi-mode cooling techniques for trapped ions, Ph.D. thesis, University of Innsbruck, 2016.

[85] O. Katz, M. Cetina, and C. Monroe, Phys. Rev. Lett. **129**, 063603 (2022).

[86] O. Katz, M. Cetina, and C. Monroe, arXiv:2207.10550 [PRX Quantum (to be published)].

[87] Z. Zhou, L.-L. Wan, and Z.-F. Xu, J. Phys. A **53**, 425203 (2020).

[88] R. T. Sutherland and R. Srinivas, Phys. Rev. A **104**, 032609 (2021).

[89] A. D. Greentree, C. Tahan, J. H. Cole, and L. C. Hollenberg, Nat. Phys. **2**, 856 (2006).

[90] P. Bienias, I. Boettcher, R. Belyansky, A. J. Kollár, and A. V. Gorshkov, Phys. Rev. Lett. **128**, 013601 (2022).

[91] D. Porras, P. A. Ivanov, and F. Schmidt-Kaler, Phys. Rev. Lett. **108**, 235701 (2012).

[92] M. Schiro, M. Bordyuh, B. Öztop, and H. E. Türeci, Phys. Rev. Lett. **109**, 053601 (2012).

[93] D. Lv, S. An, Z. Liu, J.-N. Zhang, J. S. Pedernales, L. Lamata, E. Solano, and K. Kim, Phys. Rev. X **8**, 021027 (2018).